

# Cog2 Null Mutant CHO Cells Show Defective Sphingomyelin Synthesis\*

Received for publication, May 31, 2010, and in revised form, November 2, 2010. Published, JBC Papers in Press, November 3, 2010, DOI 10.1074/jbc.M110.150011

Waldo Spessott<sup>1</sup>, Andrea Uliana<sup>1</sup>, and Hugo J. F. Maccioni<sup>2</sup>

From the Departamento de Química Biológica, Facultad de Ciencias Químicas, Centro de Investigaciones en Química Biológica de Córdoba (CIQUIBIC), Consejo Nacional de Investigaciones Científicas y Técnicas (CONICET), Universidad Nacional de Córdoba, Ciudad Universitaria, X5000 HUA Córdoba, Argentina

The COG (conserved oligomeric Golgi complex) is a Golgi-associated tethering complex involved in retrograde trafficking of multiple Golgi enzymes. COG deficiencies lead to misorganization of the Golgi, defective trafficking of glycosylation enzymes, and abnormal *N*-, *O*- and ceramide-linked oligosaccharides. Here, we show that in Cog2 null mutant IdIC cells, the content of sphingomyelin (SM) is reduced to ~25% of WT cells. Sphingomyelin synthase (SMS) activity is essentially normal in IdIC cells, but in contrast with the typical Golgi localization in WT cells, in IdIC cells, transfected SMS1 localizes to vesicular structures scattered throughout the cytoplasm, which show almost no signal of co-transfected ceramide transfer protein (CERT). Cog2 transfection restores SM formation and the typical SMS1 Golgi localization phenotype. Adding exogenous *N*-6-[(7-nitrobenzo-2-oxa-1,3-diazol-4-yl)amino]hexanoyl-4-d-erythro-sphingosine (C<sub>6</sub>-NBD-ceramide) to IdIC cell cultures results in normal SM formation. Endogenous ceramide levels were 3-fold higher in IdIC cells than in WT cells, indicating that Golgi misorganization caused by Cog2 deficiency affects the delivery of ceramide to sites of SM synthesis by SMS1. Considering the importance of SM as a structural component of membranes, this finding is also worth of consideration in relation to a possible contribution to the clinical phenotype of patients suffering congenital disorders of glycosylation type II.

Protein and lipid oligosaccharide modifying enzymes are part of a complex machinery whose individual components are asymmetrically distributed along the *cis/trans* axis of the Golgi apparatus. Asymmetry is maintained despite a continuous anterograde membrane flow that moves secretory or membrane-bound cargoes along the secretory pathway, and a continuous COPI vesicle-mediated retrograde transport that moves residents from the late to early Golgi compartment (1). Fusion of COPI vesicles with target compartments occurs with participation of intra-Golgi soluble NSF attachment pro-

tein receptors; recent evidence indicates that this fusion step is preceded by one mediated by close-range acting oligomeric or monomeric tethering factors that may confer specificity to the fusion process. Among the oligomeric tethering factors, the COG (conserved oligomeric Golgi) complex is a soluble hetero-octamer associated to the cytoplasmic surface of the Golgi complex. It has been characterized in yeast (2) and mammalian cells (3) as a tethering complex necessary for Golgi retrograde trafficking of multiple Golgi processing proteins. COG complex is constituted by eight subunits organized in two lobules, lobule A (Cog1–4) and lobule B (Cog5–8) functionally interconnected via Cog1 and Cog8 (4, 5). Immunogold electron microscopy showed Cog1-HA localizing in the proximity of the tips and rims of the Golgi cisternae, in their associated vesicles and tubulovesicular structures, and in COPI-containing vesicles (6). Structural similarities between COG complex subunits and other multimeric tether subunits, such as exocysts and Dsl1p, support a common evolutionary origin and action mechanism for these complexes (7).

In yeast, a temperature-sensitive Cog3 mutant shows defective glycosylation but nearly normal secretion kinetics associated to mislocalization of two Golgi mannosyltransferases: Och1p and Mnn1p, which lead to the suggestion that COG is involved in the distribution of Och1p in retrograde vesicles (8). In mammals, two types of CHO mutant cells deficient in the LDL receptor, IdB (Cog1 null mutant) and IdIC (Cog2 null mutant), have highly similar pleiotropic defects in processes associated to the Golgi complex and are characterized by the abnormal synthesis of *N*-linked, *O*-linked, and ceramide-linked oligosaccharides (9–13; for a review, see Ref. 14). These observations support the notion that the COG complex is a vesicle-tethering factor that normally tethers COPI retrograde transport vesicles originated in the late Golgi with *cis* Golgi membranes (15). COG also facilitates Golgi-ER traffic of some GEARs (COG-sensitive integral membrane proteins resident of the Golgi) that mislocalize and are rapidly degraded in COG mutant cells (16, 17). It has been proposed that COG and COPI participate together in the appropriate retention or recycling of GEARs and that COG prevents their accumulation in the ER and their degradation (16).

In humans, mutations in genes encoding Cog7 (18), Cog1 (19), Cog4 (20), Cog8 (21), and Cog5 (22) subunits result in congenital disorders of glycosylation type II, which characterize by defects in the processing of *N*-linked glycans. Cog7 and

\* This work was supported in part by Grant PICT 2006-01239 from Agencia Nacional de Promoción Científica y Tecnológica, Universidad Nacional de Córdoba, y MinCyT Córdoba.

<sup>1</sup> Recipients of Consejo Nacional de Investigaciones Científicas y Técnicas fellowships.

<sup>2</sup> A Career Investigator of Consejo Nacional de Investigaciones Científicas y Técnicas (Argentina). To whom correspondence should be addressed: Haya de la Torre s/n, Pabellón Argentina Ala Oeste, 5000 Córdoba, Argentina. Tel./Fax: 54-351-433-4171/4074; E-mail: maccioni@dqbc.fcq.unc.edu.ar.

*Cog1* deficient patients suffer from motor and mental retardation and die in early infancy (for a review, see Ref. 23). A *Cog8*-deficient patient also showed motor and mental retardation and showed chronic axonal neuropathy. Analysis of serum *N*-glycans from the patient evidenced normal addition of one sialic acid but severe deficiency in subsequent sialylation of mostly normal *N*-glycans (21).

In the present work, we studied the lipid composition of *ldlC* cells. Biochemical studies showed that in addition to the glycosylation defect that affect GM3 formation, a defective synthesis of sphingomyelin (SM)<sup>3</sup> also occurs in these cells. Results from enzyme activity determinations, metabolic labeling, and fluorescence microscopy indicate that reduced synthesis of SM is associated to a mislocalization of sphingomyelin synthase1 (SMS1) and defective utilization of the substrate ceramide.

## EXPERIMENTAL PROCEDURES

**Molecular Constructs**—The expression plasmid pMH2-*Cog2*-HA was a generous gift of Dr. Françoise Foulquier (Structural and Functional Glycobiology Unit UMR8576, University of Lille I). The expression plasmid for human SMS1 (SMS1-His<sub>6</sub>-V5/pcDNA3.1) (24) was a generous gift of Dr. Joost Holthuis (Utrecht University, Utrecht, The Netherlands). The expression plasmids pEGFP-C2-CERT and pEGFP-FAPP2 were a generous gift of Dr. Maria Antonietta De Matteis (Telethon Institute of Genetics and Medicine, Napoli, Italy). The expression plasmid pCFP-PH from FAPP1 was a generous gift of Dr. José Luis Daniotti Centro de Investigación en Química Biológica de Córdoba (CIQUIBIC) National University of Córdoba, Córdoba, Argentina.

**Cell Culture and Transfection**—CHO-K1 cells WT (ATCC, U.S.A.) and CHO mutant cells deficient in LDL receptor (*Cog2* null mutant, *ldlC* cells), were kindly provided by Dr. Monty Krieger (Massachusetts Institute of Technology, Cambridge, MA) (9, 11–13, 25). Cells were grown in DMEM nutrient mixture F-12 (Ham) (Invitrogen) containing 2 mM glutamine, 15 mM HEPES, 50 μg/ml penicillin, and 50 μg/ml streptomycin, supplemented with 10% fetal calf serum. At ~70% confluence, cells were transfected with 1 μg/ml of the indicated cDNA using cationic liposomes following the manufacturer's instructions (Lipofectamine, Life Technologies, Carlsbad, CA) or by electroporation of 10<sup>7</sup> cells/ml with 45 μg of total DNA using the ECM 600 electroporation system, (BTX, Genetronics, San Diego, CA) following the manufacturer's instructions.

**Fluorescence Microscopy**—Cells grown on coverslips were fixed and permeabilized for 7 min in methanol at –20 °C or fixed with paraformaldehyde 3% in PBS for 20 min and perme-

abilized with Triton X-100 0.1% of glycine (200 mM) for 10 min at room temperature. Fixed cells were incubated with the following specific antibodies: monoclonal mouse anti GM130 (1:300, BD Biosciences), monoclonal mouse anti V5 (1:500), polyclonal rabbit anti-HA (1:1000), monoclonal mouse anti-HA (1:800), polyclonal rabbit anti SMS1 (1:50, Santa Cruz Biotechnology) and appropriate secondary antibodies. Coverslips were mounted with FluorSave (Calbiochem, EMD Biosciences, Inc., La Jolla, CA) and observed under the spectral confocal microscope Olympus FluoView™ FV1000 equipped with argon multiline 458, 488, and 514 nm; helium/neon 543 nm lasers; and 100× numerical aperture 1.4 UPlanSApo oil immersion objective (Olympus). Images were compiled with Adobe Photoshop CS2. Pearson's coefficient of co-localization was calculated using ImageJ software with the JACoP plug-in (for details, see supplemental "Experimental Procedures") (26).

**Subcellular Fractionation**—WT and *ldlC* CERT-GFP transfected cells were washed three times with cold PBS and harvested by scraping in 400 μl of 5 mM Tris-HCl (pH 7.4) in the presence of protease inhibitor mixture (1:1800). After homogenization, nuclear fractions and unbroken cells were removed by centrifuging twice at 4 °C for 5 min at 600 × *g*. Supernatants were then ultracentrifuged at 4 °C for 1 h at 400,000 × *g* in an OPTIMA™ Ultracentrifuge (Beckman Coulter, Inc., Fullerton, CA). The supernatant was collected, and the pellet was resuspended in 400 μl of Tris-HCl 5 mM in the presence of protease inhibitor mixture. Protein in each fraction was precipitated with trichloroacetic acid to a final concentration of 10%, collected by centrifugation, and analyzed by SDS-PAGE and Western blot.

**Lipid Analysis**—Cells in culture (3 × 10<sup>5</sup> cells per 35-mm dish) were metabolically labeled overnight with 10 μCi/ml of D-[U-<sup>14</sup>C]galactose (329.5 mCi/mmol; DuPont NEN, Boston, MA) to label glycolipids (27) or with 10 μCi/ml of [9,10-<sup>3</sup>H]palmitic acid (53 Ci/mmol; Amersham Biosciences, Buckinghamshire, UK) to label phospholipids and ceramide. After washing with cold PBS, cells were scrapped from the plate, and lipids were extracted with chloroform:methanol (2:1 by volume) at room temperature for 30 min. Glycolipid composition was examined by HPTLC of the total lipid extract using as solvent chloroform:methanol (4:1 by volume) in a first run up to two-thirds of the plate and chloroform:methanol:0.2% CaCl<sub>2</sub> (60:36:8 by volume) in a second run up to the front of the plate. Phospholipid and ceramide composition were examined in the lower phase after a Folch partition of the lipid extract. TLC of phospholipids was carried out using chloroform:methanol:acetic acid:water (40:10:10:1 by volume) as solvent in a first run up to the front of the plate and chloroform:methanol:acetic acid:water (120:46:19:3 by volume) in a second run up to half of the plate. Unlabeled phospholipids were visualized after dipping the chromatograms in 3% cupric acetate in 8% phosphoric acid and heating at 150 °C until development of the bands. For the analysis of lower phase sphingolipids, the lower phase was saponified as follows; it was evaporated to dryness under N<sub>2</sub> in glass tubes, taken in 0.1 M KOH in methanol and either neutralized immediately or after keeping for 2 h at 37 °C with the same volume of 0.1 M HCl.

<sup>3</sup> The abbreviations used are: SM, sphingomyelin; SMS, sphingomyelin synthase; HPTLC, high performance thin layer chromatography; CERT, ceramide transfer protein; PI4K IIIβ, phosphatidylinositol 4-kinase IIIβ; PH, pleckstrin homology domain; PC, phosphatidylcholine; COPI, coat protein complex I; GM3, NeuAcα2,3Galβ1,4Glc-ceramide; CFP, cyan fluorescent protein; GFP, green fluorescent protein; FAPP1, four-phosphate adaptor protein 1; FAPP2, four-phosphate adaptor protein 2; LacCer, lactosylceramide; GlcCer, glucosylceramide; PI(4)P, phosphatidylinositol 4'-monophosphate.

## Defective Sphingomyelin Synthesis in Cog2 Null Cells

Chloroform, methanol, and water were added to achieve a Folch partition, and lipids in the lower phase were run on HPTLC. For sphingophospholipids, the solvent system was as indicated above for total phospholipids. For ceramide separation, the solvent system used was chloroform:acetic acid (9:1 (by volume)).

Lipid radioactivity in chromatograms was recorded either by phosphorimaging or by exposure to radiographic films. Densitometric quantification of chromatograms and x-ray plates were done using ImageJ (image processing and Analysis in Java) software (National Institute of Health). Liquid chromatography mass spectrometry of unlabeled lower phase lipids was carried out at the Mass Spectrometry Facility at the University of California (Riverside, CA).

**Lysenin Binding Studies**—All manipulations were done at room temperature unless noted otherwise. Cells were grown on glass coverslips in DMEM medium at 37 °C for 24 h to ~70% confluence. After washing with PBS, the cells were fixed with 3% formaldehyde in PBS for 20 min, washed with PBS, incubated with 0.1 M NH<sub>4</sub>Cl in PBS for 20 min, and washed again with PBS. After blocking with 2% BSA in PBS for 1 h, the cells were incubated with lysenin (400 ng/ml in 0.2% BSA/PBS, PeptaNova GmbH, Sandhausen, Germany) for 1 h and washed three times with PBS for 5 min with gentle shaking. Next, they were incubated with rabbit anti-lysenin antiserum (1:500 dilution in 0.2% BSA/PBS, PeptaNova GmbH) for 1 h and washed with PBS, followed by incubation with an appropriate secondary antibody. After washing with PBS, the cells were mounted and observed under a Olympus FluoView<sup>TM</sup> FV1000 confocal microscope. Confocal images of lysenin-treated WT and ldlC cells were processed with ImageJ software (National Institute of Health). First, images were converted from 12 bits to 8 bits in order to use Counting Particles ImageJ plug-in, and then the same global threshold was defined for WT and ldlC cells. 30 cells were delimited with the free region of interest (ROI) tool of the program, and particles with sizes between 0.1 and 1 μm<sup>2</sup> were counted.

**Determination of Enzyme Activities**—Homogenates of WT and ldlC cells were used as an enzyme source for determination of sialyltransferase 1 (27) and SMS (28) activities. Briefly, sialyltransferase 1 was determined in an incubation system that contained, in a final volume of 30 μl, 400 μM LacCer, 100 μM CMP[<sup>3</sup>H]NeuAc (250,000 cpm), 20 mM MnCl<sub>2</sub>, 1 mM MgCl<sub>2</sub>, 20 μg of Triton CF54/Tween 80 (2:1 w/w), 100 mM sodium cacodylate-HCl buffer (pH 6.5), and cell extract (40 μg of protein). Incubations were performed at 37 °C for 90 min. Samples without exogenous acceptor were used to discount the incorporation into endogenous acceptors. Reactions were stopped with 1 ml of 5% (w/v) trichloroacetic acid/0.5% phosphotungstic acid, and the radioactivity incorporated into lipids was determined as described (29). For determination of SMS and glucosylceramide synthase activities, the incubation system contained, in a final volume of 50 μl, 20 μM N-6-[(7-nitrobenzo-2-oxa-1,3-diazol-4-yl)amino]hexanoyl-4-d-erythro-sphingosine (C<sub>6</sub>-NBD-ceramide, Molecular Probes) complexed with bovine serum albumin in a 1:1 molar ratio, 400 μM 1-palmitoyl-2-oleoyl-*sn*-glycero-3-phosphocholine, 400 μM UDP-glucose, 5 mM MgCl<sub>2</sub>, 5 mM MnCl<sub>2</sub>, 1 mM

EDTA in 50 mM HEPES (pH 7.2), and cell homogenate (40 μg of protein). After 50 min of incubation at 37 °C, reactions were stopped by the addition of 250 μl of chloroform:methanol 2:1 (v/v) to extract C<sub>6</sub>-NBD lipids in the lower phase. After centrifugation at 1000 × g for 5 min, the lower phase was evaporated under nitrogen and subjected to TLC using chloroform:methanol:water (65:25:4, by volume) as solvent. C<sub>6</sub>-NBD lipids were visualized by UV illumination of the TLC.

**Incubation of ldlC Cells with C<sub>6</sub>-NBD-ceramide**—WT and ldlC cells were cultured 4 h in the presence of 1 μg/ml of C<sub>6</sub>-NBD-ceramide complexed with bovine serum albumin in a 1:1 molar ratio. After three washes with cold PBS, cells were harvested, and lipids were extracted with chloroform:methanol (2:1 by volume) at room temperature, and the extract was partitioned by adding 0.2 volumes of water. After centrifugation at 1000 × g for 5 min, the lower phase was evaporated under nitrogen and subjected to HPTLC by using chloroform:methanol:water (65:25:4 by volume) as solvent. C<sub>6</sub>-NBD lipids present in the chromatograms were visualized by UV illumination of the HPTLC.

**Western Blot**—For Western blot analysis, total protein from cells or cell fractions were subjected to SDS-PAGE and transferred to nitrocellulose membranes. Membranes were blocked with 5% (w/v) nonfat dried skim milk in PBS for 1 h at room temperature, followed by three 5-min washes with PBS, and reacted with the following primary antibodies: mouse monoclonal antibody anti-HA (1:1000; Sigma-Aldrich) or mouse monoclonal anti-GFP (1:2000, Roche Applied Science). Goat anti-mouse antibody coupled to IRDye 800 (1:20,000; LI-COR Biosciences, Lincoln, NE) was used as secondary antibody. Membranes were then scanned using the Odyssey IR Imager (LI-COR Biosciences, Lincoln, NE).

## RESULTS

**Lipid Composition of ldlC Cells**—Cog2 null mutant ldlC cells belong to a group of CHO mutant cells deficient in LDL receptor activity. Deficiency is due to its decreased stability as a consequence of abnormal processing of its oligosaccharides in the late stage of Golgi. ldlC cells are able to add high mannose oligosaccharides in N-linked chains to glycoproteins (LDL receptor, vesicular stomatitis virus G protein) but are unable to add sialic acid residues to these oligosaccharide chains and to convert them to completely endo-β-N-acetylglucosaminidase H-resistant forms (11). The ldlC phenotype is corrected to the CHO WT phenotype by a cDNA coding for an 83-kDa Golgi-associated, brefeldin A-sensitive peripheral protein, later on referred to as Cog2. The endogenous *LDLC* mRNA was undetectable in ldlC cells (12). To investigate the lipid composition of ldlC cells, we carried out long term metabolic labeling of total lipids of CHO WT and ldlC cells in an overnight culture with appropriate radioactive precursors. Lipids were then extracted and analyzed by TLC.

The glycolipid fraction was analyzed in the total lipid extract from cells cultured overnight in the presence of [<sup>14</sup>C]galactose. A relative accumulation of GlcCer (~1.5-fold higher than in WT cells) and LacCer (~10-fold higher than in WT cells) and a marked decrease of GM3 (~5-fold lower than in WT cells) was evident in the chromatogram (Fig. 1A).

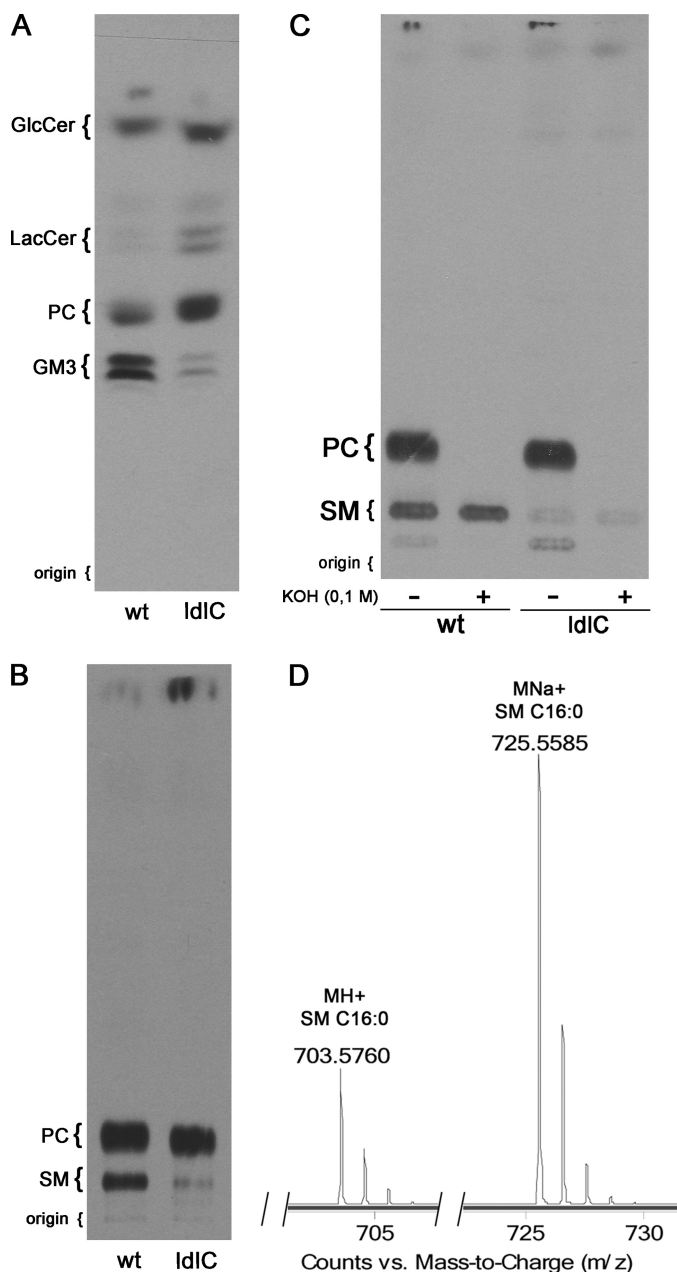


**FIGURE 1. IdIC cells show reduced sphingomyelin and GM3 content.** *A*, lipids from WT and IdIC cells cultured overnight in the presence of [ $^{14}$ C]galactose were extracted with chloroform:methanol (2:1, by volume) and total lipids separated by HPTLC as described under "Experimental Procedures." *B*, lipid extracts of cells as in *A*, but cultured with [ $^3$ H]palmitate were Folch-partitioned into a lower and an upper phase, and lipids from the lower phase were separated by TLC as indicated under "Experimental Procedures." *C*, aliquots of [ $^3$ H]palmitate-radiolabeled lipids from the lower phase of both WT and IdIC cells were subjected to mild alkaline hydrolysis as indicated under "Experimental Procedures" and then chromatographed as in *B*. The position of co-chromatographed standard lipids is shown at the left of each chromatogram. *D*, lower phase lipids from IdIC cells were separated by liquid chromatography, and the peak that eluted as the standard oleic acid containing Sphingomyelin (C18:1 SM) (elution time, 12.1 min) was subjected to mass spectrometry.

The phospholipid fraction was analyzed in the lower phase of the lipid extract from cells cultured in the presence of [ $^3$ H]palmitate, after partition against water. Compared with WT cells, IdIC cells extracts showed essentially no difference in a compound migrating as the standard phosphatidylcholine (PC) but showed a clear decrease of  $\sim 75\%$  of a compound

migrating in the chromatogram as the standard SM (Fig. 1*B*), showing that besides the defects in the glycosylation of glycolipids (11), the composition of other lipids is also affected in IdIC cells.

**IdIC Cells Have Reduced Sphingomyelin Content**—To identify the compound running as SM and partially missing from IdIC cells, the lower phase lipids of both WT and IdIC cells, were subjected to mild alkaline hydrolysis. If, as suspected, this compound is SM, it should be resistant to saponification, whereas the major glycerophospholipid PC should not. It is clear in Fig. 1*C* that after alkaline hydrolysis, the bands running as PC in both WT and IdIC cells completely disappeared, whereas the bands running as SM remained intact, indicating that the compound is not a glycerolipid and most probably is SM. A liquid chromatography mass spectrometric analysis of lower phase lipids from WT and IdIC cells confirmed that the compound eluted from the liquid chromatograph at the time at which a standard sample of oleic acid containing Sphingomyelin (C18:1 SM) elutes (12.1 min) shows ions at  $m/z$  703.6 and 725.56, corresponding to the protonated and Na adduct of 16:0 SM, respectively (Fig. 1*D*). The quantification of the SM content in radioactive samples derived from long term metabolic labeling from [ $^3$ H]palmitate was confirmed by direct measurement of SM mass in lipid extracts from both cell types. For this, lower phase lipids from WT and IdIC cells were separated by TLC, and stained lipid bands were quantified by densitometry. The SM content in IdIC cells lipid extract was  $\sim 65\%$  lower than in WT cells (supplemental Fig. 1), consistent with  $\sim 75\%$  lower content determined from metabolic labeling experiments.

**IdIC Cells Show Reduced Lysenin Aggregates at Plasma Membrane**—Lysenin is a pore-forming toxin from the earthworm *Eisenia foetida* that specifically binds SM clusters in membranes (30, 31). To see whether the decreased total SM content in lipid extracts of IdIC cells (Fig. 1) affects cell surface SM expression, the binding of lysenin was determined in fixed IdIC cells. By confocal microscopy, it was found that IdIC cell plasma membrane shows less lysenin aggregates than WT cells (Fig. 2*A*). Quantification of these aggregates indicates that although  $\sim 70\%$  of the WT cells show between 10 and 40 aggregates per cell, most IdIC cells show  $< 10$  aggregates (Fig. 2*B*), thus showing that the level of plasma membrane SM is also affected in IdIC cells.

**Sphingomyelin Synthase Activity Is Comparable in WT and IdIC Cells**—SM is synthesized in the Golgi complex by SMS1, a multipass membrane protein of the Golgi, and by SMS2, a plasma membrane protein. Both enzymes catalyze the transfer of phosphocholine moiety of PC to the acceptor ceramide to synthesize SM (24), but SMS1 acts as a major SM synthase activity (32). Recent immunoelectron microscopy data revealed that SMS1 was mostly present at the *trans* side of the Golgi of HeLa cells (33). We determined this activity in homogenates of WT and IdIC cells by measuring the conversion of the exogenous fluorescent ceramide analog  $C_6$ -NBD-ceramide into fluorescent SM (Fig. 3*A*). Quantitative estimation of the formed product revealed that the SMS activity in IdIC cells was essentially

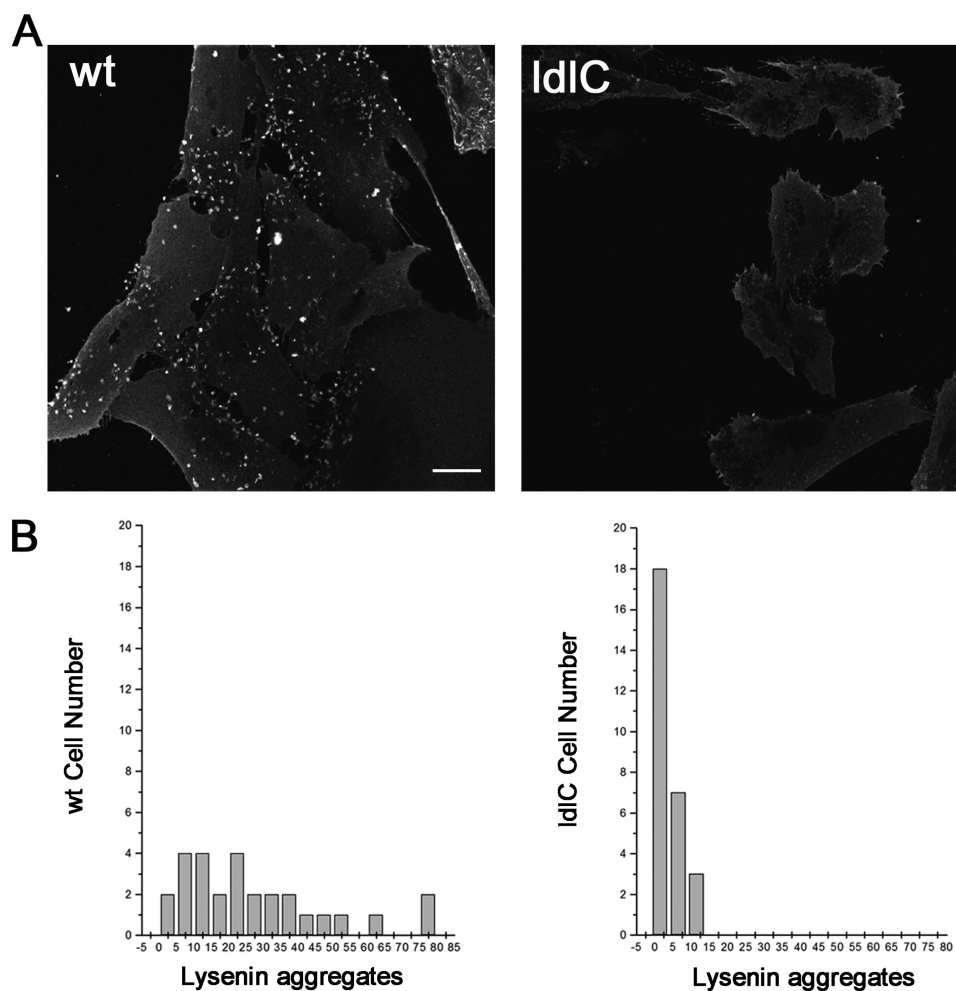


FIGURE 2. **Lysenin binding reveals decreased levels of plasma membrane SM in IdlC cells.** A, WT and IdlC CHO cells were fixed, treated with lysenin at room temperature for 1 h, and then treated with anti-lysenin antiserum followed by the fluorescent secondary antibody. Cells were observed in a confocal microscope. B, the number of lysenin aggregates per cell was determined by counting 30 cells in each condition using ImageJ software, as indicated under "Experimental Procedures." Scale bar, 10  $\mu$ m.

as in WT cells (Fig. 3A). Formation of GlcCer, the product of glucosylceramide synthase activity also measured in the assay, was slightly increased in IdlC cells but the difference was not significant (Fig. 3A).

*Incubation of IdlC Cells with  $C_6$ -NBD-ceramide Results in Normal Formation of  $C_6$ -NBD-sphingomyelin*—The fact that in SM-defective IdlC cells the *in vitro* activity of SMS1 is essentially normal (Fig. 3A) suggests that *in vivo*, some of the two participating substrates of the SM synthesis reaction, PC, and/or ceramide, may be not available to SMS1. To test this possibility and considering that the PC level was normal in IdlC cells (Fig. 1B), they were tested for their capacity to incorporate exogenous  $C_6$ -NBD-ceramide into SM when cultured in its presence. This fluorescent ceramide analog permeates the cellular membranes and accumulates in intracellular structures, concentrating particularly in the Golgi complex (34); it has been suggested that this is due to its trapping in the lumen as a consequence of the addition of the phosphorylcholine head group in the conversion into SM by Golgi SMS activity (32). Fig. 3B shows the HPTLC analysis of the lower phase of a lipid extract from these cells. The percentage of fluorescent SM

relative to the total fluorescent products formed was essentially the same in WT and IdlC cells. GlcCer formation from  $C_6$ -NBD-ceramide was also similar in both cells. This result indicates that SMS is catalytically active also *in vivo* provided the substrate ceramide is given exogenously, suggesting that other factors may be affecting the normal supply of endogenous ceramide to SMS1.

*IdlC Cells Have Increased Ceramide Content*—The results of Fig. 3B suggest that reduced SM synthesis in IdlC cells may be the consequence of reduced ceramide levels in these cells. To investigate this possibility, WT and IdlC cells were cultured overnight in the presence of [ $^3$ H]palmitic acid, and the level of endogenous ceramide was determined after HPTLC separation of the alkali-resistant fraction of the lower phase lipids. Contrary to what was expected, the ceramide level in IdlC cells was found increased  $\sim$ 3-fold with respect to WT cells (Fig. 4). Direct measurement of ceramide mass in lipid extracts from both cells types gave essentially the same value of increase in favor of IdlC cells (supplemental Fig. 2). The simplest interpretation of this experiment is that reduced ceramide content is not the cause for the reduced level of SM in IdlC cells. Rather, the increase suggests a reduced consumption of ceramide due to the block in SM synthesis.

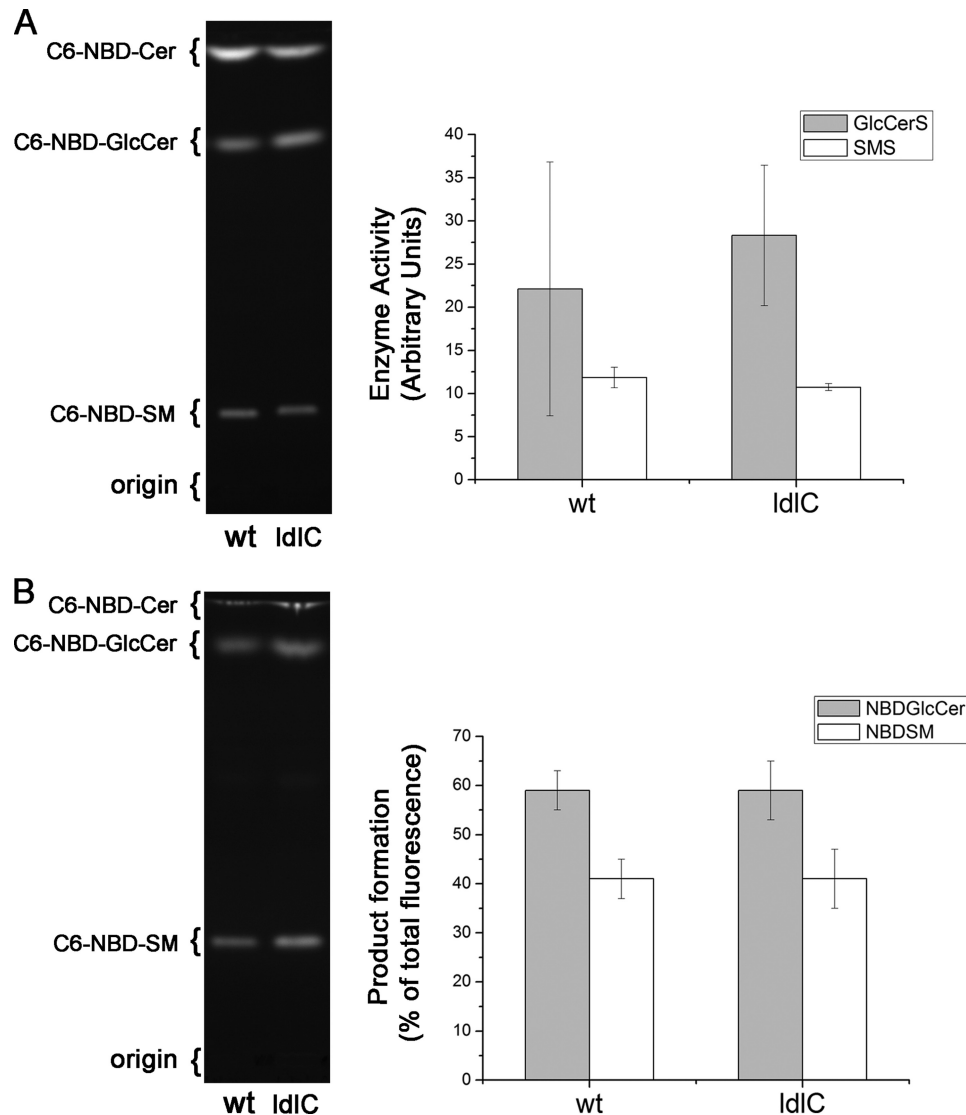


FIGURE 3. *In vitro* SMS activity and *in vivo* C<sub>6</sub>-NBD-ceramide utilization. *A*, homogenates of WT and IdIC cells were assayed for the activities of SMS and glucosylceramide synthase in conditions of linearity with time and protein concentration. Lipids were extracted from incubates, separated by HPTLC, and formed fluorescent compounds visualized under UV light illumination. Quantification was carried out by densitometry of the fluorescent bands using ImageJ software. Enzyme activity values are given as mean arbitrary fluorescent units  $\pm$  S.D. for three independent experiments. Other details were as described under "Experimental Procedures." *B*, C<sub>6</sub>-NBD-ceramide (*Cer*) utilization in IdIC cells. WT and IdIC cells monolayers were cultured in the presence of 1  $\mu$ g/ml C<sub>6</sub>-NBD-ceramide for 4 h. Cells were harvested, and lipids were extracted and separated by HPTLC. Formed fluorescent compounds were photographed under UV light illumination, and the percent contribution of the bands quantified by densitometry using ImageJ software. For *A* and *B*, the positions of lipid standards are indicated at the left of the chromatogram.

*IdIC* Cells Show Altered Subcellular Localization of SMS—Considering the possibility that the structural misorganization of the Golgi complex of IdIC cells (35) may affect the coupling of biochemical reactions leading to SM formation, the localization of SMS1 was examined in these cells. WT and IdIC cells were transfected with V5-tagged SMS1, and the subcellular localization was compared with that of the endogenous Golgi marker GM130, a Cog-insensitive protein (16). Whereas in  $90 \pm 2\%$  of WT cells, SMS1-V5 and the Golgi marker GM130 localized in typical perinuclear, Golgi-like structures (Fig. 5A), only  $14 \pm 4\%$  of IdIC cells showed SMS1 with the typical Golgi perinuclear localization. Instead, in most IdIC cells, a considerable fraction of SMS1 localizes in vesicular structures scattered throughout the cytoplasm. The difference in localization is most im-

pressive when the endogenous SMS1 was immunostained with a specific antibody (Fig. 5B). Co-transfection of IdIC cells with *Cog2* cDNA, re-established the localization of SMS1-V5 to a pattern characteristic of the Golgi complex in  $88 \pm 4\%$  of the co-transfected cells (Fig. 5C); *Cog2*-HA itself was just slightly concentrated in the Golgi region, at variance with the typical Golgi localization of endogenous COG complex subunits. It was already reported for overexpressed *Cog1*-HA that it also localizes to the ER without impairment of its function (19). These results point to SMS1 mislocalization due to *Cog2* absence as a possible cause of the observed defective SM synthesis.

*Cog2* Transfection Restores SM Levels of IdIC Cells to Near Normal Values—If the reduced SM content of IdIC cells actually results from *Cog2* deficiency, transfecting *Cog2*

## Defective Sphingomyelin Synthesis in *Cog2* Null Cells

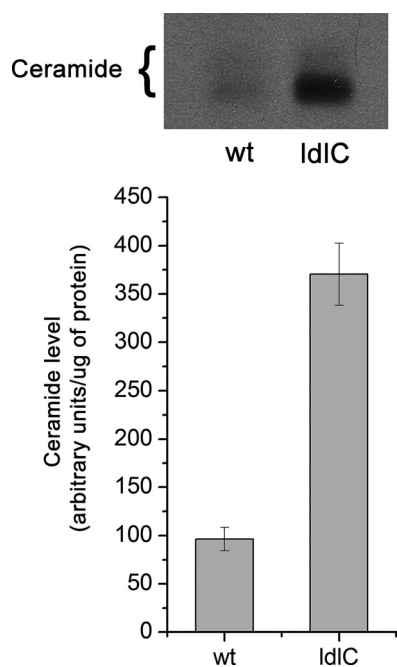


**FIGURE 4. IdIC cells show increased ceramide levels.** Lipids from WT and IdIC cells cultured overnight in the presence of [9,10- $^3$ H]palmitic acid were extracted with chloroform:methanol (2:1, by volume) and Folch-partitioned into a lower and an upper phase. Lower phase lipids were subjected to mild alkaline hydrolysis and partitioned, and the chloroform phase was separated by TLC using chloroform:acetic acid (9:1, by volume). Other details were as described under "Experimental Procedures."

cDNA to IdIC cells should revert the SM-deficient phenotype. Cells were transfected with *Cog2*-HA, and 24 h after transfection, they were pulsed overnight with [ $^3$ H]palmitate. Transfection was verified by Western blot, which showed *Cog2*-HA protein present in the transfected cell population (Fig. 6A). Lipids were extracted from WT, mock transfected, and transfected IdIC cells, separated as in Fig. 1B, and the PC to SM ratio was determined by densitometric scanning of the x-ray autoradiograms. In two independent experiments, nontransfected IdIC cells show a SM/PC labeling ratio of  $\sim 0.1$ , which was reverted to  $\sim 0.20$  upon transfection with *Cog2* (Fig. 6B). Determination of the SM mass in the alkali-resistant lower phase lipids of these cells gave similar values of increase ( $\sim 1.8$  fold) in the SM content in *Cog2*-HA-transfected IdIC cells with respect to nontransfected IdIC cells (supplemental Fig. 3). These values were  $\sim 50\%$  of the corresponding value in WT cells, but because in our hands, the efficiency of transfection is  $\sim 40\%$ , the values indicate that SM synthesis was practically restored in *Cog2*-transfected IdIC cells. Taken together, the results of Figs. 5 and 6 and supplemental Fig. 3 indicate a close causal relationship between *Cog2* deficiency, SMS1 mislocalization, and SM synthesis deficiency.

**CERT and SMS1 Localize to Different Membranes in IdIC Cells**—Ceramide for SM synthesis is synthesized in the ER and transported from the ER to the *trans* Golgi, where it is converted to SM. The cytosolic protein CERT mediates the ER-to-Golgi trafficking of ceramide. It has been suggested that CERT extracts ceramide from the ER and transfers it to the Golgi apparatus in a nonvesicular manner at close apposi-

tion sites between the ER and the Golgi apparatus membranes (36). It is possible that in IdIC cells with abnormal Golgi organization, CERT binding and ceramide delivery to SMS1-containing compartments do not operate properly. To address this point, WT and IdIC cells were transfected with a GFP-tagged version of CERT, and 18 h later, cells were fixed and observed under a confocal microscope. As described previously (37), CERT was found concentrated in the perinuclear region of  $\sim 75\%$  of WT cells (Fig. 7A). Conversely, most IdIC cells show that CERT is distributed throughout the cytoplasm. Only 23% of IdIC cells show CERT concentrated in vesicular structures dispersed in the cytoplasm, reminiscent of Golgi fragments (Fig. 7A). Determination of the amount of CERT-GFP in the supernatant and membrane-bound fractions of WT and IdIC cells by Western blot, evidenced that the membrane bound fraction of CERT in IdIC cells relative to the unbound fraction, was lower than in WT cells (0.33 versus 0.82, respectively) (Fig. 7C). As shown in Fig. 5, A and B, most SMS1 also localize to vesicular structures scattered throughout the cytoplasm in IdIC cells (Fig. 7B). To investigate whether SMS1 and CERT co-localize in the vesicular structures, WT and IdIC cells were co-transfected with CERT-GFP and SMS1-V5, fixed with paraformaldehyde, permeabilized with Triton X-100, and observed under the microscope. This procedure may allow the release of a fraction of the cytoplasmic CERT-GFP (see Fig. 7C) and hence explain the apparent lower fluorescence in cells of Fig. 7B with respect to Fig. 7A. Results indicate that most of the membranes containing SMS1 in IdIC cells do not bind CERT. Only 17.8% of co-transfected IdIC cells show CERT and SMS1 partially co-localizing in vesicular structures (Pearson's coefficient =  $0.58 \pm 0.04$ ). A deficit of PI(4)P in membranes containing SMS1 in IdIC cells is probably the cause of reduced CERT binding, but if so, the deficit is selective for SMS1-containing structures because the binding of a GFP-tagged version of FAPP2 (four-phosphate adaptor protein 2), that is also mediated by PI(4)P was essentially as in WT cells, with the fluorescence concentrated in perinuclear Golgi-like structures in both cells (Fig. 7A) (see "Discussion"). In addition, examining the localization of PI(4)P by visualizing the localization of transfected FAPP1-PH-CFP (Fig. 7A, cyan), shows that in WT cells, the binding occurs mainly in the Golgi region marked by GM130 (red). On the other hand, in IdIC cells, a wide subcellular distribution of PI(4)P is observed. Even so, a faint specific binding of FAPP1-PH-CFP (cyan) in the Golgi region marked by GM130 (red) is still observed.

## DISCUSSION

*Cog2* null mutant IdIC cells are CHO cells characterized by having deficient LDL receptor activity due to its decreased stability associated to the abnormal processing of its oligosaccharides in the late Golgi (11). This phenotype was corrected by a cDNA coding for an 83-kDa Golgi-associated, brefeldin A-sensitive peripheral protein, referred to as *Cog2* (12). Subsequent work, led to the identification of mutations in different proteins of the COG complex in patients with congenital disorders of glycosylation type II (13).

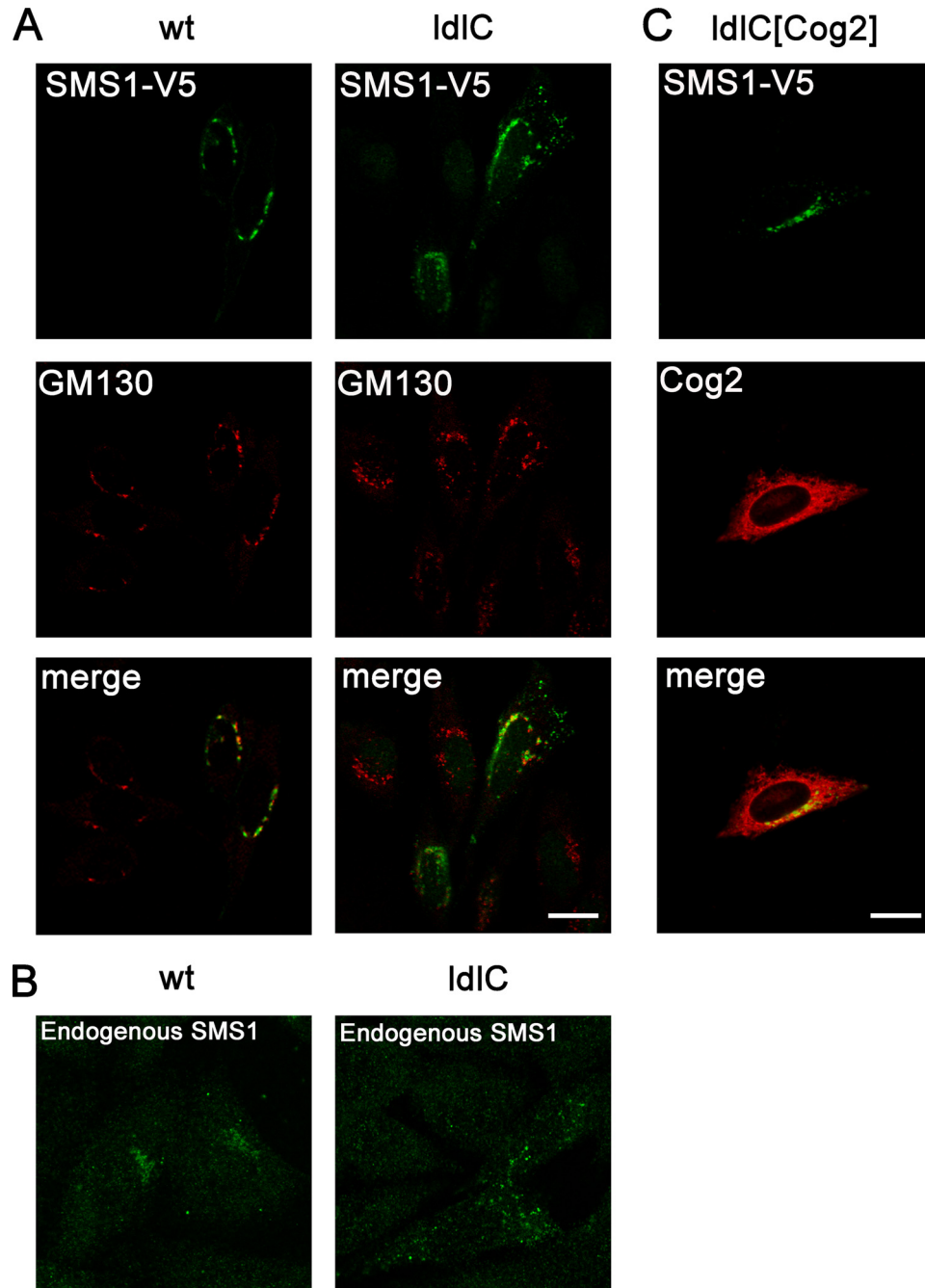


FIGURE 5. **Cog2** transfection restores Golgi localization of SMS1 in IdIC cells. *A*, WT and IdIC cells transiently expressing SMS1-V5 were immunostained with appropriated antibodies for V5 tag (green) and the endogenous *cis* Golgi marker GM130 (red). Data were obtained from three independent experiments, each with  $n = 50$  cells. *B*, endogenous SMS1 was immunostained with its specific antibody, and controls without primary antibody for WT and IdIC cells were made. Phenotype observed in three independent experiments, each with  $n = 100$  cells. *C*, IdIC cells transiently co-expressing SMS1-V5 (green) and Cog2-HA (red) were immunostained with the appropriated antibodies. Data were obtained from three independent experiments, each with  $n = 30$  cells. Scale bar, 10  $\mu\text{m}$ .

We have examined the lipid composition of IdIC cells, with particular attention to members of the phospholipid family and have found that a lipid compound identified as SM was decreased to  $\sim 25\%$  of WT cells (Fig. 1*B*) and that such a reduction is also detectable at the plasma membrane level by measuring the binding of lysenin (Fig. 2). Noticeably, the enzyme activity of SMS in cell homogenates was similar in WT and IdIC cells (Fig. 3*A*) and also was similar in the metabolic conversion of exogenous  $C_6$ -NBD-cera-

mid into  $C_6$ -NBD-SM (Fig. 3*B*). Lack of endogenous ceramide was discarded as the main cause for the defective synthesis of SM because ceramide was found increased 3-fold in IdIC cells (Fig. 4).

SM synthesis is mainly catalyzed by SMS1, although a plasma membrane-localized SMS2 also contributes to total cellular SM synthesis (24, 32). Fine ultrastructural localization studies in HeLa cells mapped the residence of SMS1 to the *trans* cisternae of the Golgi (33). Microscopic examina-



## Defective Sphingomyelin Synthesis in *Cog2* Null Cells

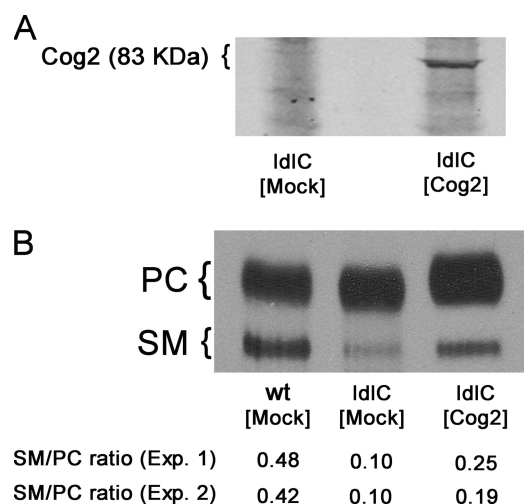


**FIGURE 6. *Cog2* cDNA transfection increases SM level of IdIC cells.** *A*, IdIC cells were transfected with *Cog2* cDNA, and the expression of *Cog2* (83 KDa) was visualized by Western blot using anti-HA monoclonal antibody in both mock-transfected and *Cog2*-transfected cells, as indicated. *B*, transfected IdIC cells were cultured overnight in the presence of [<sup>3</sup>H]palmitate. Radioactive lipids from mock-transfected WT and IdIC cells and from *Cog2*-transfected IdIC cells (*IdIC [Cog2]*) were extracted with chloroform:methanol (2:1, by volume), the extract was partitioned, and the lower phase was analyzed by HPTLC as described under "Experimental Procedures." Chromatograms were exposed to radiographic films, and the percent contribution of the bands was quantified by densitometry using ImageJ software. The SM/PC ratio determined for each cell type in two independent experiments (Exp. 1 and Exp. 2) is indicated at the *bottom* of the autoradiogram.

tion of transfected SMS1-V5 to WT CHO cells showed this enzyme in a compact perinuclear distribution comparable with that of the Golgi marker GM130. However, in IdIC cells, SMS1-V5 was found in vesicular structures scattered throughout the cytoplasm (Figs. 5*A* and 7*B*). *Cog2* transfection was effective in restoring SMS1 localization to the Golgi (Fig. 5*C*) and also in restoring the SM synthesis level to nearly normal levels in IdIC cells metabolically labeled with [<sup>3</sup>H]palmitate (Fig. 6).

Altogether, these results strongly suggest that structural alterations of the Golgi complex associated to the *Cog2* deficiency in IdIC cells restrict proper coupling between SMS1 and its substrates. Because IdIC cells show an increased level of ceramide (Fig. 4), no difference in PC content with respect to WT cells, and metabolic conversion of exogenous C<sub>6</sub>-NBD-ceramide into SM was essentially as in WT cells, results point to a failure in the usage of endogenous ceramide by SMS1.

Ceramide for SM synthesis is transported from the ER to the Golgi by a nonvesicular mechanism involving the cytoplasmic ceramide transfer protein CERT (37). Disruption of Golgi morphology of HeLa cells by the microtubule-de stabilizing agent nocodazole reduced SM synthesis by ~50% (38). This was attributed to disruption of zones of close proximity between membranes of *trans* ER *trans* Golgi used by CERT for delivery of ceramide for synthesis of SM. However, dispersion of the Golgi seems not to be an obvious cause of defective SM synthesis, because ilimaquinone, which also promotes Golgi disorganization, does not affect SM synthesis (38).

The morphological alterations of the *trans* Golgi region in *Cog2*-deficient IdIC cells, where SMS1 resides (33), are remi-

niscant of the effects of the pharmacological agents mentioned above. We found CERT concentrated in the Golgi region of the majority of WT cells, but only in 23% of IdIC cells (Fig. 7*A*), the majority of which present CERT mainly spread throughout the cytoplasm. When CERT was co-expressed with SMS1 in IdIC cells, both proteins were found localized to vesicular structures in the cytoplasm; however, they scarcely co-localize in these structures (Fig. 7*B*). CERT is targeted to the Golgi by the binding to PI(4)P, present in Golgi membranes, through its PH domain. Among several possibilities for the lack of co-localization, one is that SMS1-containing structures are topologically segregated from those bearing CERT-binding capacity; another possibility is that SMS1-containing membranes have particularly reduced PI(4)P content. PI(4)P synthesis depends on PI4K III $\beta$  activation by protein kinase D (39), which is in turn activated by diacylglycerol. As diacylglycerol is a by-product of SMS1 activity, diacylglycerol and consequently PI(4)P may be reduced in these membranes, affecting binding of CERT, but this deserves further investigation.

IdIC cells show a slight accumulation of GlcCer, a marked accumulation of LacCer and a reduced content of GM3 (Fig. 1*A*) (11). These results indicate that the supply of ceramide for GlcCer synthesis and the coupling of GlcCer for LacCer synthesis are not heavily affected in IdIC cells, if at all affected. FAPP2 mediates the delivery of GlcCer from proximal to distal Golgi where LacCer synthesis occurs (40), or to the ER where it enters the secretory pathway and then reaches the Golgi lumen for further elongation to LacCer (33). Transfected FAPP2 show a perinuclear staining in a majority of WT and IdIC cells (Fig. 7*A*), indicating that localization of FAPP2 is not heavily affected. FAPP2 binds GlcCer and PI(4)P at the Golgi complex by its glycolipid transfer protein and PH domains, respectively (40). Therefore, we cannot distinguish whether FAPP2 was localized to the Golgi via binding to PI(4)P or via binding to GlcCer. In addition, because the existence of PI4K III $\beta$  and the binding of the PH domain of FAPP1 in proximal Golgi membranes was reported (41; for a review, see Ref. 42), the possibility also exists that the binding of FAPP2 that we observed occurred on proximal Golgi membranes. In fact, determination of PI(4)P levels by examining the localization of FAPP1-PH-CFP evidenced a major fraction of the probe spread over the cytoplasm, and also a detectable fraction localizing to the Golgi region of IdIC cells. Thus, at difference with CERT that is mainly spread in the cytoplasm (Fig. 7*A*), both FAPP2 and FAPP1-PH-CFP localization assays suggest the existence of an available PI(4)P pool, presumably in proximal Golgi membranes, which may allow the extraction of GlcCer by FAPP2 and therefore the provision of GlcCer for LacCer synthesis (33, 40). The marked increase of LacCer and reduction of GM3 and the essentially normal activity of sialyltransferase 1, which converts LacCer into GM3 in IdIC cells (43), suggests that the compartment containing sialyltransferase 1 in IdIC cells is either unable to acquire LacCer for further sialylation to GM3 or does not provide the optimal milieu for the reaction to occur.

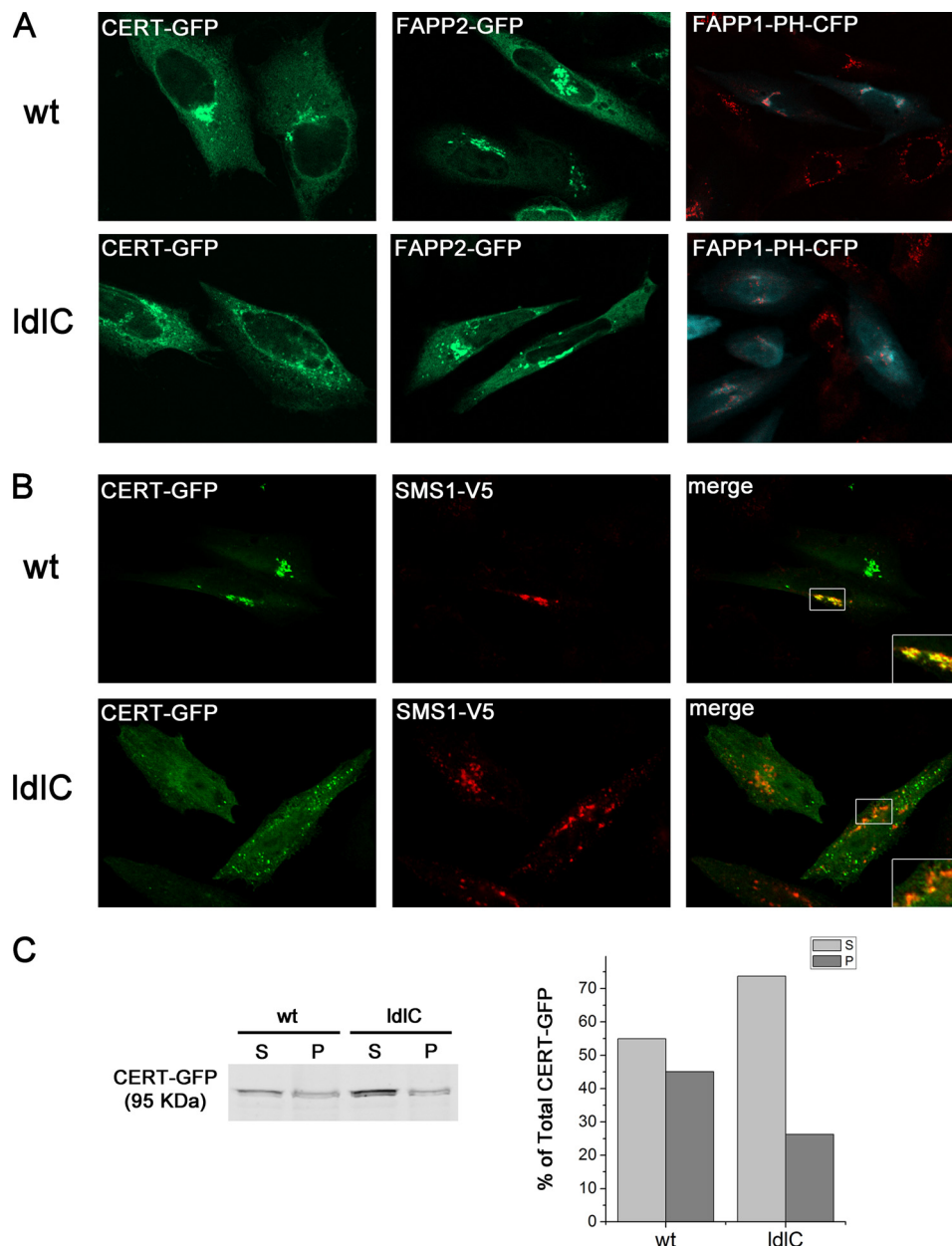


**FIGURE 7. CERT, SMS1, FAPP2, and FAPP1-PH domain localization in WT and IdIC cells.** *A*, CERT-GFP and FAPP1-PH-CFP but not FAPP2-GFP localization are altered in IdIC cells. WT and IdIC cells were transfected with CERT-GFP (green), FAPP2-GFP (green) or transfected with FAPP1-PH-CFP (cyan) and stained for the endogenous Golgi marker GM130 (red). Cells were fixed and observed under a confocal microscope. *B*, CERT and SMS1 localized to different membranes in IdIC cells. WT and IdIC cells were co-transfected with CERT-GFP and SMS1-V5. Cells were fixed with 3% paraformaldehyde in PBS for 20 min and permeabilized with Triton X-100 0.1% glycine (200 mM) for 10 min at room temperature and immunostained with monoclonal mouse anti-V5 and the appropriate secondary antibody conjugated with Alexa Fluor 546. WT cells show significant co-localization (Pearson's coefficient =  $0.86 \pm 0.05$ ), whereas IdIC cells only show partial co-localization (Pearson's coefficient =  $0.58 \pm 0.04$ ) between CERT and SMS1 in three independent experiments, with each analyzing 30 cells. *Insets* are a higher magnification of the boxed areas in the cells. *C*, WT and IdIC CERT-GFP-transfected cells were homogenized, and supernatant (S) and pellet (P) fractions were obtained by ultracentrifugation at  $400,000 \times g$  as described under "Experimental Procedures."

Although it is well established that defects in glycan terminal glycosylation observed in congenital disorders of glycosylation type II disorders can be ascribed to late Golgi dysfunction, it is less clear whether the clinical phenotype of the patients results only from the abnormal glycosylation pattern of membrane-bound or secreted glycoconjugates or whether other products requiring a functional late Golgi for their synthesis may add to this phenotype. SM has important cell biological implications as a structural component of plasma membranes and plasma membrane

microdomains (44) and as co-regulator of cholesterol homeostasis (45). In addition, its synthesis by SMS1 modulates the cellular levels of diacylglycerol and ceramide, which are lipid messengers involved in the control of cell proliferation (32, 46). Therefore, defective levels of SM and imbalances of diacylglycerol to ceramide ratios may be considered as potential contributors to the clinical phenotype of patients with congenital disorders of glycosylation type II. Future investigation will be needed to understand how IdIC cells cope with the affected SM synthesis.

**Acknowledgments**—We thank Javier Valdez-Taubas and Mariana Ferrari for critical reading of the manuscript. We also thank Gabriela Schachner and Susana Deza for technical assistance with cell cultures and Carlos Mas and María Cecilia Sampedro for assistance with confocal microscopy.

### REFERENCES

- Bonifacino, J. S., and Glick, B. S. (2004) *Cell* **116**, 153–166
- Whyte, J. R., and Munro, S. (2002) *J. Cell Sci.* **115**, 2627–2637
- Ungar, D., Oka, T., Krieger, M., and Hughson, F. M. (2006) *Trends Cell Biol.* **16**, 113–120
- Ungar, D., Oka, T., Brittle, E. E., Vasile, E., Lupashin, V. V., Chatterton, J. E., Heuser, J. E., Krieger, M., and Waters, M. G. (2002) *J. Cell Biol.* **157**, 405–415
- Oka, T., Vasile, E., Penman, M., Novina, C. D., Dykxhoorn, D. M., Ungar, D., Hughson, F. M., and Krieger, M. (2005) *J. Biol. Chem.* **280**, 32736–32745
- Vasile, E., Oka, T., Ericsson, M., Nakamura, N., and Krieger, M. (2006) *Exp. Cell Res.* **312**, 3132–3141
- Richardson, B. C., Smith, R. D., Ungar, D., Nakamura, A., Jeffrey, P. D., Lupashin, V. V., and Hughson, F. M. (2009) *Proc. Natl. Acad. Sci. U.S.A.* **106**, 13329–13334
- Bruinsma, P., Spelbrink, R. G., and Nothwehr, S. F. (2004) *J. Biol. Chem.* **279**, 39814–39823
- Krieger, M., Brown, M. S., and Goldstein, J. L. (1981) *J. Mol. Biol.* **150**, 167–184
- Krieger, M., Reddy, P., Kozarsky, K., Kingsley, D., Hobbie, L., and Penman, M. (1989) *Methods Cell Biol.* **32**, 57–84
- Kingsley, D. M., Kozarsky, K. F., Segal, M., and Krieger, M. (1986) *J. Cell Biol.* **102**, 1576–1585
- Podos, S. D., Reddy, P., Ashkenas, J., and Krieger, M. (1994) *J. Cell Biol.* **127**, 679–691
- Chatterton, J. E., Hirsch, D., Schwartz, J. J., Bickel, P. E., Rosenberg, R. D., Lodish, H. F., and Krieger, M. (1999) *Proc. Natl. Acad. Sci. U.S.A.* **96**, 915–920
- Sztul, E., and Lupashin, V. (2009) *FEBS Lett.* **583**, 3770–3783
- Shestakova, A., Zolov, S., and Lupashin, V. (2006) *Traffic* **7**, 191–204
- Oka, T., Ungar, D., Hughson, F. M., and Krieger, M. (2004) *Mol. Biol. Cell* **15**, 2423–2435
- Stee, R., and Kornfeld, S. (2006) *Mol. Biol. Cell* **17**, 2312–2321
- Wu, X., Stee, R. A., Bohorov, O., Bakker, J., Newell, J., Krieger, M., Spaapen, L., Kornfeld, S., and Freeze, H. H. (2004) *Nat. Med.* **10**, 518–523
- Foulquier, F., Vasile, E., Schollen, E., Callewaert, N., Raemaekers, T., Quelhas, D., Jaeken, J., Mills, P., Winchester, B., Krieger, M., Annaert, W., and Matthijs, G. (2006) *Proc. Natl. Acad. Sci. U.S.A.* **103**, 3764–3769
- Reynders, E., Foulquier, F., Leão Teles, E., Quelhas, D., Morelle, W., Rabouille, C., Annaert, W., and Matthijs, G. (2009) *Hum. Mol. Genet.* **18**, 3244–3256
- Kranz, C., Ng, B. G., Sun, L., Sharma, V., Eklund, E. A., Miura, Y., Ungar, D., Lupashin, V., Winkel, R. D., Cipollo, J. F., Costello, C. E., Loh, E., Hong, W., and Freeze, H. H. (2007) *Hum. Mol. Genet.* **16**, 731–741
- Paesold-Burda, P., Maag, C., Troxler, H., Foulquier, F., Kleinert, P., Schnabel, S., Baumgartner, M., and Hennet, T. (2009) *Hum. Mol. Genet.* **18**, 4350–4356
- Foulquier, F. (2009) *Biochim. Biophys. Acta* **1792**, 896–902
- Huitema, K., van den Dikkenberg, J., Brouwers, J. F., and Holthuis, J. C. (2004) *EMBO J.* **23**, 33–44
- Kingsley, D. M., and Krieger, M. (1984) *Proc. Natl. Acad. Sci. U.S.A.* **81**, 5454–5458
- Bolte, S., and Cordelieres, F. P. (2006) *J. Microscopy* **244**, 213–232
- Daniotti, J. L., Landa, C. A., and Maccioni, H. J. (1994) *J. Neurochem.* **62**, 1131–1136
- Veldman, R. J., Mita, A., Cu villier, O., Garcia, V., Klappe, K., Medin, J. A., Campbell, J. D., Carpentier, S., Kok, J. W., and Levade, T. (2003) *FASEB J.* **17**, 1144–1146
- Daniotti, J. L., Landa, C. A., Rösner, H., and Maccioni, H. J. (1991) *J. Neurochem.* **57**, 2054–2058
- Yamaji, A., Sekizawa, Y., Emoto, K., Sakuraba, H., Inoue, K., Kobayashi, H., and Umeda, M. (1998) *J. Biol. Chem.* **273**, 5300–5306
- Yamaji-Hasegawa, A., Makino, A., Baba, T., Senoh, Y., Kimura-Suda, H., Sato, S. B., Terada, N., Ohno, S., Kiyokawa, E., Umeda, M., and Kobayashi, T. (2003) *J. Biol. Chem.* **278**, 22762–22770
- Tafesse, F. G., Huitema, K., Hermansson, M., van der Poel, S., van den Dikkenberg, J., Uphoff, A., Somerharju, P., and Holthuis, J. C. (2007) *J. Biol. Chem.* **282**, 17537–17547
- Halter, D., Neumann, S., van Dijk, S. M., Wolthoorn, J., de Mazière, A. M., Vieira, O. V., Mattjus, P., Klumperman, J., van Meer, G., and Sprong, H. (2007) *J. Cell Biol.* **179**, 101–115
- Lipsky, N. G., and Pagano, R. E. (1985) *J. Cell Biol.* **100**, 27–34
- Zolov, S. N., and Lupashin, V. V. (2005) *J. Cell Biol.* **168**, 747–759
- Hanada, K., Kumagai, K., Tomishige, N., and Yamaji, T. (2009) *Biochim. Biophys. Acta* **1791**, 684–691
- Hanada, K., Kumagai, K., Yasuda, S., Miura, Y., Kawano, M., Fukasawa, M., and Nishijima, M. (2003) *Nature* **426**, 803–809
- Chandran, S., and Machamer, C. E. (2008) *Traffic* **9**, 1894–1904
- Fugmann, T., Hausser, A., Schöffler, P., Schmid, S., Pfizenmaier, K., and Olayioye, M. A. (2007) *J. Cell Biol.* **178**, 15–22
- D'Angelo, G., Polishchuk, E., Di Tullio, G., Santoro, M., Di Campli, A., Godi, A., West, G., Bielawski, J., Chuang, C. C., van der Spoel, A. C., Platt, F. M., Hannun, Y. A., Polishchuk, R., Mattjus, P., and De Matteis, M. A. (2007) *Nature* **449**, 62–67
- Weixel, K. M., Blumental-Perry, A., Watkins, S. C., Aridor, M., and Weisz, O. A. (2005) *J. Biol. Chem.* **280**, 10501–10508
- D'Angelo, G., Vicinanza, M., Di Campli, A., and De Matteis, M. A. (2008) *J. Cell Sci.* **121**, 1955–1963
- Spessott, W., Uliana, A., and Maccioni, H. J. (2010) *Neurochem. Res.*, in press
- Van der Luit, A. H., Budde, M., Zerp, S., Caan, W., Klarenbeek, J. B., Verheij, M., and Van Blitterswijk, W. J. (2007) *Biochem. J.* **401**, 541–549
- Ridgway, N. D. (2000) *Biochim. Biophys. Acta* **1484**, 129–141
- Hannun, Y. A., and Obeid, L. M. (2002) *J. Biol. Chem.* **277**, 25847–25850